ELSEVIER

Journal of Nuclear Materials 270 (1999) 154–164

journal of nuclear materials

The effects of adsorbates on Zircaloy oxidation in air and steam

Kwangheon Park [a,*], Yoonchol Cho [b], Yun-Goo Kim [c]

[a] *Center for Advanced Reactor Research, Institute of Materials Science and Technology, Department of Nuclear Engineering, Kyunghee University, Suwon, South Korea*

[b] *Korea Nuclear Fuel Ltd., Yusong-Gu, Taejon 305-600, South Korea*

[c] *Sam Chang Enterprise Ltd., 889-3 Kuangyang-Dong, Dongar-Gu, Anyang, South Korea*

Received 26 May 1998; accepted 10 December 1998

Abstract

The effects of adsorbates on the oxidation of Zircaloy-4 in air and steam are studied by the measurement of the weight gain of specimens. The effect of LiOH is dependent on surface condition, temperature and type of atmosphere. LiOH works as a mineralizer stabilizing monoclinic phases. LiOH only affects the specimens of pickled surface. LiOH enhances oxidation at low temperature, but retard oxidation at high temperature. NaCl enhances the oxidation, where nonuniform stresses on the surface and embrittlement of oxide by Cl are the cause. The effects of fluorides on oxidation are also measured. NaF is most harmful and KF follows next. LiF does not effect the oxidation of Zry.

1. Introduction

Zircaloy (Zry) cladding is the first protective barrier against the release of radioactive fission products from the fuel during normal and accidental conditions. The oxidation of Zry has been of great concern due to its importance on the safety of nuclear reactors. Zry oxidation has been widely investigated in water [1–7] and steam environments [8–12]; however, relatively little data exist for the oxidation in air [13]. Spent nuclear fuels contain more than 96% of fissionable materials, and are considered as energy resources in the future. Spent fuels are stored in both wet and dry methods. Nowadays, dry storage facilities are more favored because of lower operation cost, improved safety margin in criticality, and easier selection of available sites. However, the spent fuel temperature in the dry storage facility is higher than that in wet storage. So, corrosion and creep of spent fuels are important topics for the safety of dry storage facilities.

The air oxidation of Zry cladding has been an interesting topic, but there exist relatively small amount of the experimental data. And, some adsorbates are possible to stay on the surface of fuel claddings during dry storage. For example, LiOH, a pH-controller in the coolant of Pressurized Water Reactor (PWR), can be an adsorbate. NaCl also can be adsorbed on the surface of fuels from the permeated air near the sea during storage. And, organic dirt may be on the fuel surface. However, the roles of these adsorbates have not been clarified, so far.

The integrity of cladding is an important issue, during the accident of a nuclear reactor as well as the normal operation. NRC regulations indicate the maximum cladding oxidation during the accident, as that the calculated total oxidation of the cladding shall nowhere exceed 0.17 times the total cladding thickness before oxidation. In the severe accident case like LOCA, Zry claddings with H_3BO_3 and LiOH adsorbed on the surface are oxidized in steam rather than clean Zry claddings. However, the effects of these adsorbates on the steam-oxidation of Zry cladding have not been studied, so far. In this paper, the effects of these adsorbates on the oxidation of Zry in steam and air are mentioned, and

* Corresponding author. Tel.: +82-331 280 2558; fax: +82-331 281 4965; e-mail: kpark@nms.kyunghee.ac.kv

0022-3115/99/$ – see front matter
PII: S0022-3115(98)00903-9

the possible mechanisms of these adsorbates are also discussed.

2. Experimental

The oxidation rates of Zry claddings were determined by measuring the weight-gain of the specimen. Both of intermittent and continuous measurements were used in the experiment. The intermittent method of measuring weight gain was used in the experiments at the low temperatures (<500°C), while continuous measurements were done at temperatures, 700–900°C. The specimens are commercial Zircaloy-4 tubes, as-received fresh Westinghouse products used in Kori PWR power plants. The elemental composition of Zircaloy-4 is in Table 1. The tubes were cut and pickled to be used as specimens (height ~1 cm). We used the pickling method given in ASTM G2-88 [14].

In the air oxidation experiments, two types of adsorbed specimens were prepared: specimens with adsorbates on the pickled surface and those on the oxide layer that was prepared before adsorption. In the case of LiOH and NaCl, both types of specimens were made and tested. Fluorides (LiF, NaF and KF) representing possible dirt on the fuel surface were tested in the latter case only. Adsorption of these adsorbates is done by drying after the insertion of specimens in 1 M solution for an hour at room temperature. Experiments were done at three temperatures, 400, 450, and 500°C. The specimens are oxidized in the air with 80% relative humidity (referenced at room temperature).

The average surface concentration of each adsorbate was measured by redissolving the adsorbate on a specimen in water after drying. The concentration of the adsorbate in a bottle of water containing a specimen was measured by ICP. The average surface concentration was obtained from total amount of adsorbate in a bottle of solution and the specimen surface area. The results are shown in Table 2.

In the steam oxidation of Zry claddings, LiOH and boric acid are used as adsorbates. The sample preparation method is identical with those used in air oxidation experiments. Specimens adsorbed with LiOH and the mixture of H_3BO_3 and LiOH on the pickled surface were tested. The mixture of H_3BO_3 and LiOH were made from the solution containing equal molar amount of these compounds. Experiments were performed at temperatures from 700°C to 900°C.

Table 2
The average surface concentration of adsorbates on the specimens. Ox: adsorbate on the oxide surface, Me: on metal surface

Adsorbate	Average surface concentration (mg/m^2)
LiOH	2.4(±15%)(Ox)/3.5(±15%)(Me)
NaCl	5.0(±10%)(Ox)/5.3(±15%)(Me)
NaF	3.9(±10%)(Ox)
KF	5.8(±10%)(Ox)
LiF	1.2(±30%)(Ox)

3. Results

3.1. Adsorbates on the pickled surface in air oxidation

Zry specimens without adsorbates on the surface were oxidized intermittently and the results are shown in Fig. 1. The results are compared with those of Suzuki and Kawasaki (dashed lines) [13]. The experimental data (points and solid lines) are very close to those of Suzuki and Kawasaki (dashed lines). Transition points at 450 and 500°C are noticeable during the measurement period. While the color of post-transition oxide of Zry formed in steam or water looks white, most specimens oxidized in air take the color of (bright) yellowish brown. Even the white oxide formed in steam turns into yellowish brown, when Zry is reoxidized in air. The oxide formed in air may contain small amount of ZrN, the color of which is yellowish brown. However, we could not detect its existence by XRD or Raman spectrometer analyses.

The adsorbate, LiOH enhances the oxidation of Zry in air (Fig. 2). Two repeated-experimental results are collected and shown all together in Fig. 2. The oxidation rate is high initially; but after a transition point, the rate decreases. It is not clear whether the trend of the decreased oxidation rate continues; but, seems to have another transition at 500°C during the measurement period. There appears large deviation in weight gain results after the transition.

Table 1
Elemental composition of Zircaloy-4

Alloying addition	Sn	Fe	Cr	Ni	Total Fe,Cr,Ni
Zircaloy-4 (w/o)	1.50 (1.20–1.70)	0.20 (0.18–0.24)	0.10 (0.07–0.13)	<0.007	>0.28

Maximum impurity Levels														
Element	Al	B	Cd	C	Co	Cu	Hf	H	Mn	Mn	N	Si	Ti	W	U
Ppm	75	0.5	0.5	270	20	50	200	25	50	50	80	200	50	100	3.5

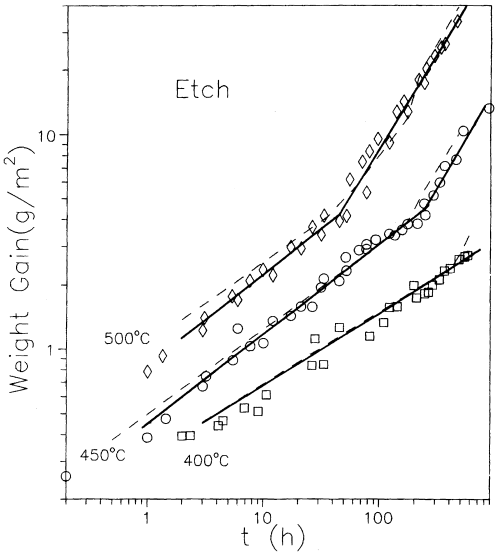

Fig. 1. The weight gain of etched specimens.

NaCl also enhances the oxidation of Zry (Fig. 3). There are some deviations in weight gain measurements between two repeated experiments, which may come from the concentration difference of NaCl adsorbed on the surface. The transition points do not appear during the measurement. The oxidation follows approximately the parabolic rate law.

The oxidation rate can be expressed as follows:

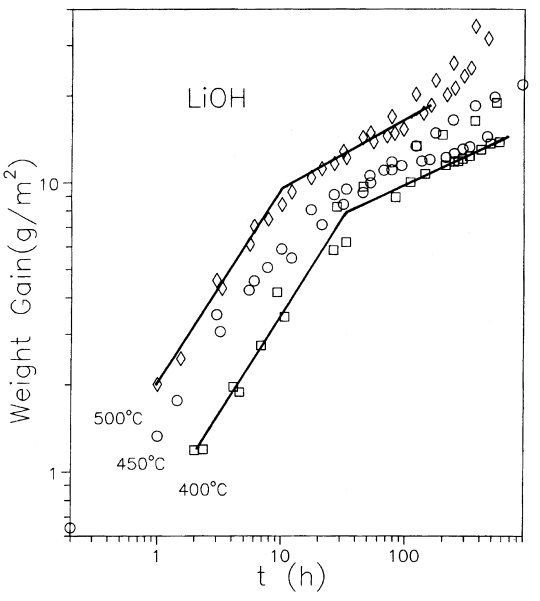

Fig. 2. The weight gain of Zry with LiOH adsorbed on the etched surface.

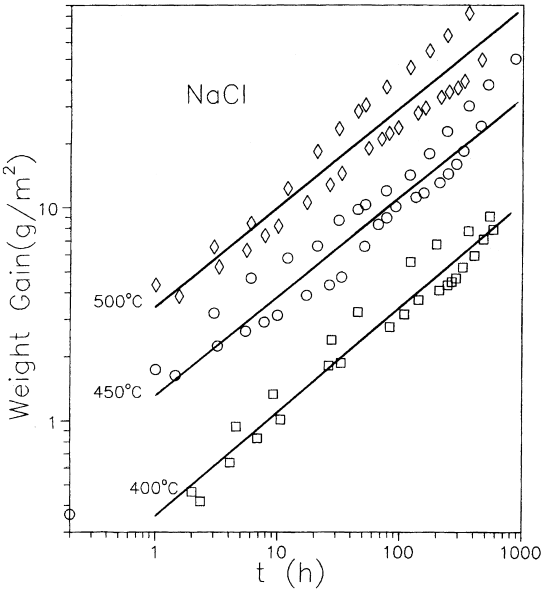

Fig. 3. The weight gain of Zry with NaCl adsorbed on the etched surface.

$$\text{Pre-transition:} (\Delta W)^n = K_n\ t$$

$$\text{Post-transition:} (\Delta W - \Delta W_t)^m = k_m(t - t_t),$$

where n, m, K_n, K_m are experimentally measured kinetic constants, ΔW_t is weight gain at the transition point, and t_t is transition time. Table 3 shows the kinetic constants for the oxidation of etched, LiOH- and NaCl-adsorbed specimens. The unit of weight gain is g/m^2.

Fig. 4 shows the weight gains of all three types of specimens based on Table 3. Open and close symbols indicate experimental results at 400 and 500°C, respectively. Both LiOH and NaCl adsorbed on the surface enhance the oxidation of Zry. NaCl affects more actively with the increase of temperature than LiOH does.

3.2. Adsorbates on the oxide surface in air oxidation

The role of adsorbates staying on the oxide layer was examined by putting adsorbates on the surface after the oxide layer formed. Fig. 5 shows the experimental results. Clean Zry specimens are oxidized in air up to 5 g/m^2 (post-transition region) at 500°C, then pulled out and immersed in the solution containing the adsorbates. After adsorption, the specimens are reoxidized at a fixed temperature. The temperature was 450°C in the case of Fig. 5. Adsorbed NaCl enhances the oxidation of Zry, while enhancement of LiOH on oxidation is negligible. Adsorbed LiOH seems to affect only the formation of initial oxide on the Zry surface. Fluoride except LiF enhances oxidation more than NaCl does. NaF is a most

Table 3
Kinetic constants for the oxidation of etched, LiOH- and NaCl-adsorbed specimens

Specimen	Temp (°C)	n	K_n	t_t	ΔW_t	m	K_m
Zry	500	2.36	0.657	44.9	4.195	1.07	0.092
	450	2.38	0.153	245.6	4.606	1.01	0.017
	400	2.95	0.0321	N.A.	N.A.	N.A.	N.A.
LiOH-Zry	500	1.42	2.59	9.2	9.2	4.1	963
	400	1.44	0.56	32.8	8.0	5.1	1316
NaCl-Zry	500	2.04	13.9	N.A.	N.A.	N.A.	N.A.
	450	2.14	1.78	N.A.	N.A.	N.A.	N.A.
	400	2.32	0.123	N.A.	N.A.	N.A.	N.A.

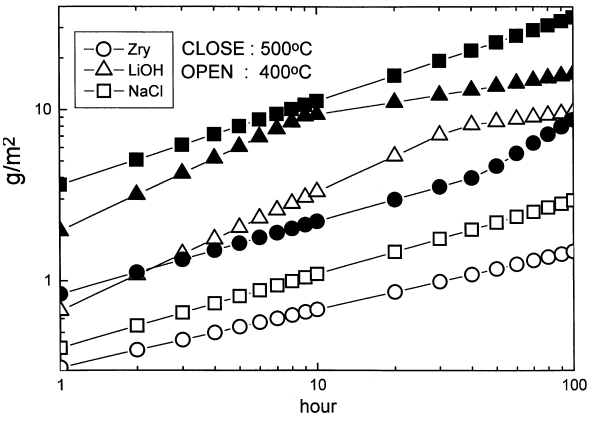

Fig. 4. Comparison of weight gains of Zry, LiOH adsorbed Zry, and NaCl adsorbed Zry specimens.

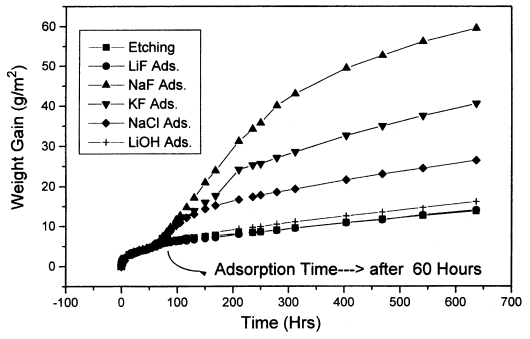

Fig. 5. The effects of adsorbates on the air oxidation, when Zry specimens with oxide layer are adsorbed. Adsorbates are LiOH, NaCl, LiF, KF, and NaF.

harmful adsorbate, and KF is the next. LiF does not influence Zry oxidation.

3.3. Adsorbates in steam oxidation

Specimens adsorbed by LiOH and those by the mixture of H_3BO_3 and LiOH on the pickled surface were oxidized in steam, to see the effects of the chemicals used in the primary system on the steam oxidation of Zry at the high temperature ($T > 700$°C). The adsorbate mixture of both H_3BO_3 and LiOH were made from the solution containing equal molar amount of each compound. The experiments were done at temperatures from 700°C to 900°C. Fig. 6 shows the results at near 900°C. Continuous measurement results are shown in open symbols. LiOH slightly retards the steam oxidation of Zry, while the mixture of LiOH and H_3BO_3 gives negligible effect on the oxidation. All three specimens (Zry, LiOH on Zry, mixture of LiOH and H_3BO_3 on Zry) identically prepared as those used in the continuous method, were simultaneously oxidized in steam to eliminate possible errors during the measurement. Weight gain of each specimen (880, 890°C) during the experiment is also shown in Fig. 6 (solid symbols). We can still see the slight retarding effect of LiOH on steam oxidation at high temperature. The mixture of H_3BO_3 and LiOH does not make any noticeable effect.

The effect of LiOH on steam oxidation of Zry at 450°C was also measured in 1 atm steam. Fig. 7 shows the experimental results. Air-oxidation results are also shown for the comparison. Contrary to the retarding role at the high temperature, LiOH at this temperature enhances the oxidation of Zry, however, the extent of

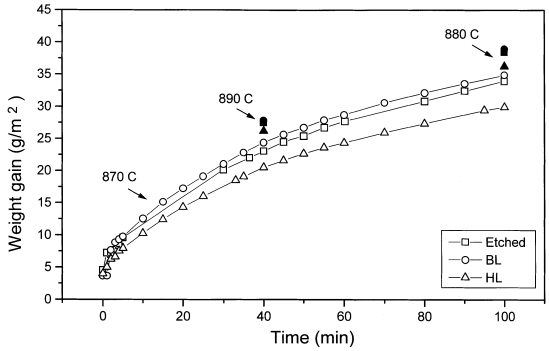

Fig. 6. Effects of LiOH and the mixture of LiOH and H_3BO_3 on steam oxidation of Zry at high temperatures. □: Etched surface, Δ: LiOH, O: H_3BO_3 + LiOH.

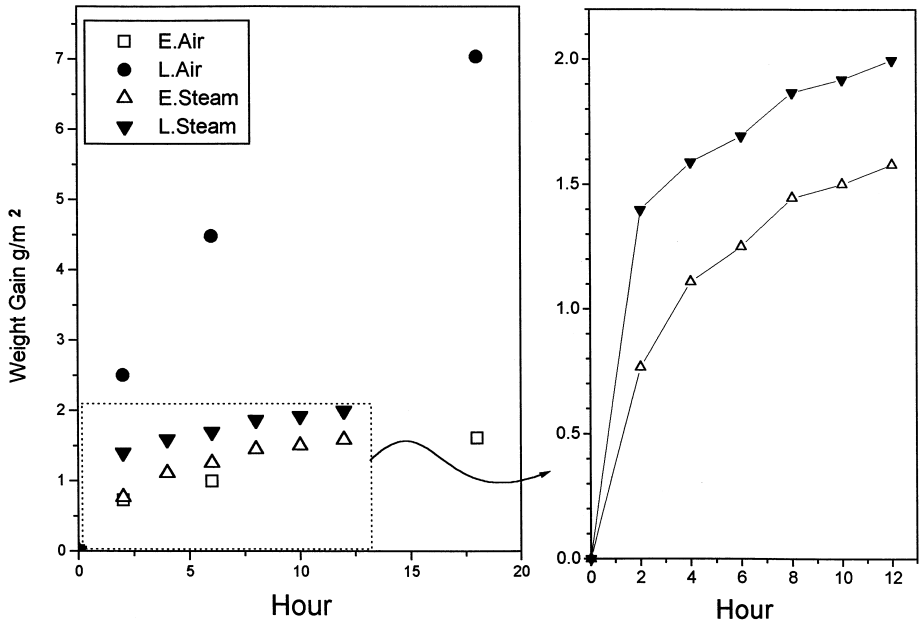

Fig. 7. LiOH effect on oxidation of Zry in steam at 450°C. E and L mean Zry with clean surface and Zry adsorbed by LiOH, respectively. Steam and air indicate the atmosphere.

effect is quite smaller than that in air oxidation. LiOH looks like affecting oxidation only at the initial stage.

4. Discussion

The role of LiOH on the corrosion of Zry in the primary system of PWR has been an important topic, due to the acceleration of corrosion rate in the presence of high concentration of LiOH. Hillner and Chirigos found the corrosion resistance was significantly reduced at the concentration of LiOH corresponding to pH 11.7 and higher. They interpreted these phenomena as the increase of anion vacancy concentrations in oxygen-deficient zirconia due to Li dopants [15]. Ramasubramanian and Balakrishnan insist that the enhancement of corrosion is caused by O–Li groups on the surface and oxide grains, since these O–Li groups retard the diametral and columnar grain growth, resulting in a fine-grained oxide and the enhanced corrosion rate [16]. Cox suggests the dissolution of cubic/tetragonal zirconia in the pores, where the solution concentration is locally high, causes enhanced corrosion by the formation of a porous inner layer of oxide [17]. Pecheur and Godlewski found the oxide layer formed on the metal–oxide interface is equiaxed and smaller, when the strong enhancement of the oxidation rate occurs in LiOH solution [18].

The roles of LiOH on the oxidation of Zry in air and in steam are similar to that in solution. Fig. 8 shows a brief summary of the experimental results of LiOH effects on Zry oxidation in these atmospheres. LiOH enhances the oxidation at the low temperature (<500°C). LiOH affects only the initial oxide formation, so is the corrosion rate. LiOH in air oxidation is more effective than in steam. However, LiOH decreases the oxidation rate at the high temperature (>700°C). Interestingly, H_3BO_3 retards this role of LiOH.

The oxidation rate of Zry in air at the lower temperature, when LiOH is adsorbed on the pickled surface of Zry, is very high up to a transition point, then the rate decreases. Fig. 9 shows the surface of specimens just after LiOH adsorption on the etched surface (Fig. 9(a)),

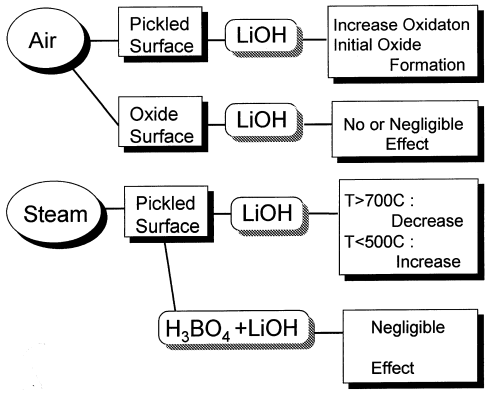

Fig. 8. A brief summary of the results of the effects of LiOH on Zry oxidation in air and in steam.

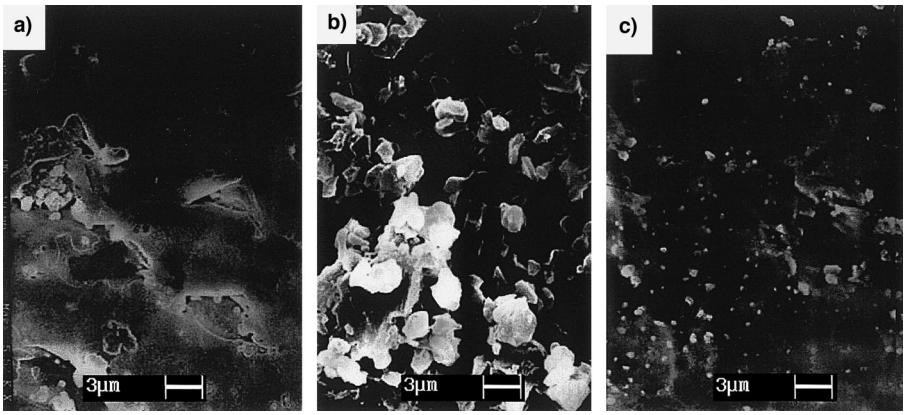

Fig. 9. The surface of LiOH adsorbed Zry, (a) after adsorption, (b) 30 h at 450°C, (c) 736 h at 500°C

30 h oxidation at 450°C (Fig. 9(b)), and 736 h oxidation at 500°C (Fig. 9(c)) in air. Fine powders (or crystals) of $LiOH \cdot n(H_2O)$ are adsorbed on the surface, not uniformly. When it is heated, these powders conglomerate to form small particles. Thermodynamically, the formation of Li_2ZrO_3 on the surface is possible [19], but we could not detect its existence by Raman spectroscopy. After a long period of oxidation, the conglomerates totally disappear and porous oxide surface shows up. Based on the evaporation feature of these conglomerates, they are suspected as LiOH.

LiOH is known to work as a mineralizer during corrosion in high temperature water. Concentrated LiOH in liquid solution makes the initial oxide layer very fine structure enough to oxidize abnormally fast. Ramasubramanian insists O–Li groups on the oxide surface impede the diametral and columnar growth of oxide crystallites resulting in fine-grained oxide and an enhanced corrosion rate [16,20]. Garzarolli suggested that LiOH cause a smaller grain size in the oxide and a more rapid transition from the tetragonal oxide phase to the monoclinic phase [21]. The role of LiOH as a stabilizer of monoclinic oxide phase during the oxidation in air also can be found in this study. Fig. 10 shows the Raman spectra of Zry oxide specimens prepared in different conditions – firstly, oxide on clean pickled surface: (a) 1.76 g/m^2 in air at 450°C, (b) 5.28 g/m^2 in air at 450°C, (c) 6.13 g/m^2 in steam at 450°C, secondly, oxide on LiOH adsorbed surface: (d) 2.13 g/m^2 in air at 450°C. Thin oxide layer (Fig. 10(a), 1.2 μm) formed on pickled surface of Zry in air mainly consists of tetragonal zirconia. Even though the spectrum contains high level of noise, the signal from monoclinic oxides is almost absent. With the growth of oxide, monoclinic phases start showing up (Fig. 10(b), 3.6 μm; Fig. 10(c), 4.2 μm). These oxides are in the post-transition growth region. The difference in spectrum is hardly noticeable between these two, even though the oxidizing atmosphere is quite different. Still, we can detect the tetragonal phases in the

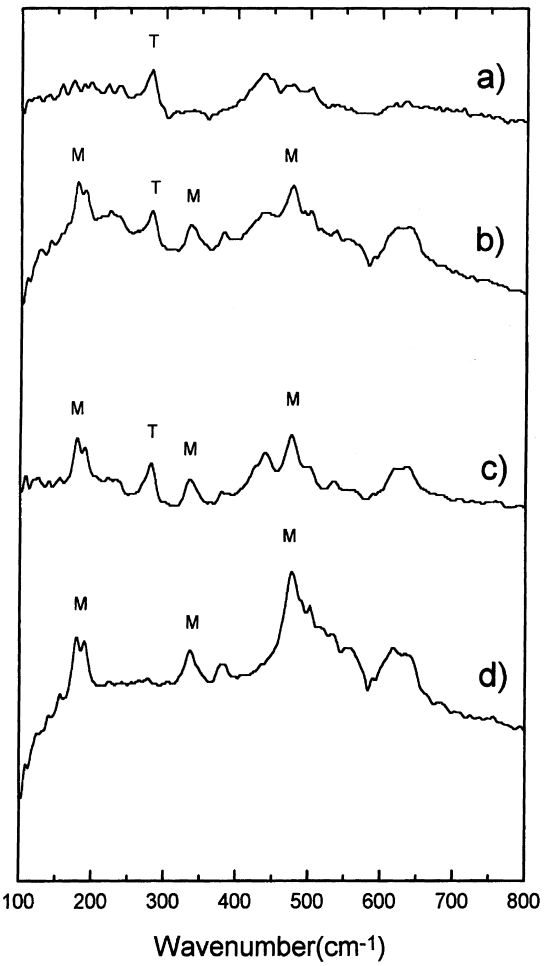

Fig. 10. Raman spectroscopy of the oxide surface. (a) p.s., 1.76 g/m^2 in air at 450°C, (b) p.s., 5.28 g/m^2 in air at 450°C, (c) p.s., 6.13 g/m^2 in steam at 450°C, (d) l.s., 2.13 g/m^2 in air at 450°C, where p.s. and l.s. mean oxides formed on pickled surface and on LiOH adsorbed surface, respectively.

post-transition oxide layer. The oxide formed on LiOH adsorbed Zry in air (Fig. 10(d), 1.4 μm) does not show any tetragonal phase. Considering tetragonal phases are observed in the thick post-transition oxide, it is interesting that this thin oxide formed on LiOH adsorbed surface does not show any tetragonal phase. It means LiOH stabilizes monoclinic phases during oxidation in air.

When oxide forms on the Zry substrate, compressive stress appears in the oxide layer due to the high value of Pilling–Bedworth ratio (ca. 1.57) [22,23]. Thermodynamically, the stability of tetragonal phase is a function of pressure and temperature, and tetragonal oxides can exist at high compressive stress below 1000°C [24]. Based on TEM analysis, Garzarolli observed that an oxide layer formed in oxygen had a higher proportion of tetragonal oxide than an oxide formed in steam or water, due to the missing effect of hydrogen which accelerates the allotropic transformation [7]. This can be a possible explanation why tetragonal phases were mainly observed in Raman spectroscopy of the thin oxide layer formed in air (Fig. 10(a)). At the low temperature, oxygen diffusion is mainly through fast paths (grain boundaries, dislocations) [26,27]. LiOH stabilizes monoclinic oxides and seems to change the oxide structure in such a way that the oxides formed by adsorbed LiOH supply much more fast paths to oxygen than the normal oxides do, so enhance the oxidation initially.

Anada suggests a three-layer oxide structure, i.e., monoclinic oxides over tetragonal oxides, and tetragonal oxides over the substoichiometric Zr oxide layer just above the metal substrate, during the pre-transition period in steam oxidation [25]. Assuming this three-layer structure be applicable, the main difference in the oxide structure formed in steam and that in air is the portion of monoclinic phases in the oxide layer. Oxides formed in steam should contain a higher portion of monoclinic phases [7]. Experimental results indicate the oxidation rate of Zry in air is almost equal to (or, somewhat slower than) that in steam or water [6,13] in the pre-transition region. The oxygen vacancy diffusion coefficient of tetragonal zirconia is known to be an order higher than that of monoclinic zirconia, based on the parabolic rate coefficient of each phase [30–32]. This means the oxides formed in air should be more tightly joined during the pre-transition period, so fast diffusion paths are less developed than in steam.

In this study, LiOH enhances oxidation much more noticeably in air than in steam. LiOH has a equilibrium vapor pressure about 10^{-6} bar at 450°C in air or in steam [28,29], so there always be a possibility of the movement of LiOH vapor to the inner oxide. The enhanced oxidation of LiOH adsorbed Zry in air can be explained in the following way. In air oxidation, LiOH vapor attacks the tightly joined tetragonal oxide layer and makes locally small monoclinic oxides. This local rapid transformation increases fast diffusion paths to oxygen, and also the oxidation rate. However, the role of LiOH as a monoclinic stabilizer in steam oxidation is quite weaker than in air, due to the existence of hydrogen that also accelerates the allotropic transformation. So, the LiOH effect on oxidation in steam is not so strong as in air oxidation. This acceleration effect cannot continue since LiOH cannot reach to tetragonal phase as the oxide thickens. When LiOH is adsorbed on the specimen after the formation of thick oxide layer, the oxidation rate is rarely affected (Fig. 5). Most oxides eligible to contact LiOH already exist as the stable monoclinic phase, and LiOH cannot change the oxide structure, or the oxidation rate.

LiOH slightly retards the oxidation at the high temperature (>700°C). The effect is small, but noticeable. Fig. 11 shows the surface of the specimens tested at 870°C. The oxide surface of Zry tube without adsorption (Fig. 11(a)) shows a normal surface with cracks originated from thermal shock. Fine spherical oxide grains appear on the surface of LiOH-adsorbed Zry (Fig. 11(b)). In the case of adsorption of the mixture of H_3BO_3 and LiOH, the fine grains appear locally (where LiOH seem concentrated locally), and microcracks are shown in between (Fig. 11(c)). It is not clear whether these microcracks are from the thermal shock or exist originally.

Contrary to the active research on the tetragonal oxides during the low temperature corrosion, the stability of tetragonal phases at high temperature oxidation is hardly studied. Generally, oxide films formed below 1000°C have been considered as monoclinic zirconia only. However, Lightstone and Pemsler observed both monoclinic and tetragonal zirconia in the oxide growing at 920°C by an in situ X-ray analysis [33,34]. So, there is a possibility that the three layer oxide structure [24] exists at the high temperature (700–1000°C). If tetragonal oxides in the oxide layer contribute oxygen diffusion in this temperature range, the rate-controlling step would be the diffusion through the monoclinic oxide layer due to the lower oxygen mobility in the monoclinic phase. LiOH on Zry surface stabilizes monoclinic oxides during oxidation, and the rate controlling monoclinic oxide layer can be easily and fully developed. Due to the early and fully developed monoclinic oxides, the oxidation rate decreases in the case of LiOH adsorbed Zry at the high temperature.

LiOH works as a mineralizer, which makes nonuniform transformation of tetragonal to monoclinic oxides. So is true at the high temperature, since the fine oxide grains is also observable at the oxide surface of LiOH adsorbed Zry (Fig. 11(b)). LiOH enhances oxidation at the low temperature, due to the increased oxygen fast-paths. At high temperatures, oxidation mechanism is somewhat different. The contribution of bulk diffusion

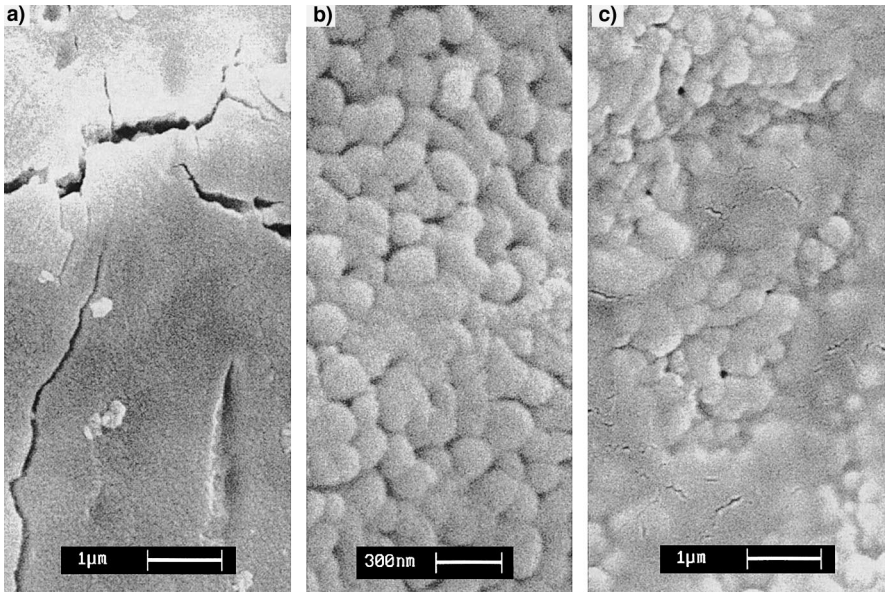

Fig. 11. The oxide surface of Zry specimens at 870°C for 100 min in steam; (a) without adsorption, (b) LiOH adsorption, (c) adsorption of the mixture of H_3BO_3 and LiOH.

becomes important, as are the oxide types (monoclinic or tetragonal). Hart and Chaklader observed that oxygen-deficient zirconia has superplasticity at high temperatures and the tetragonal-monoclinic inversion is not destructive in oxygen-deficient zirconia [35]. Due to this superplasticity of oxygen-deficient zirconia near metal interface, fast-diffusion paths may not be generated so much at the high temperature as at the low temperature during phase transformation.

Interestingly, H_3BO_3 also interrupts the role of LiOH on oxidation at the high temperature. H_3BO_3 seems to make LiOH distributed locally and not uniformly. Oxidation rate should be faster in the LiOH-free region (or H_3BO_3 region). As monoclinic phases grow in the LiOH region, they compress nearby thicker oxide located in the H_3BO_3 region, resulting in microcrack formation in nearby oxide. This may be the reason why the microcracks are observable just in between locally distributed LiOH region (Fig. 11(c)). If these microcracks form in growing oxide, they certainly enhance oxidation, since they supply open paths to oxygen or steam to inner oxide. The oxidation rate of Zry adsorbed by the mixture of LiOH and H_3BO_3 is equal to or slightly superior to that of normal Zry.

The oxidation of specimens NaCl-adsorbed on the pickled surface approximately follows a parabolic rate law. Fig. 12 shows the specimen surface after adsorption (Fig. 12(a)) and the surface after 36 h oxidation at 450°C (Fig. 12(b)). Several size salt crystals are shown on the surface. When oxidation begins, cracks start to show up just around salt crystals. Cracks surrounding big salt crystals are frequently observed (Fig. 12(b)).

Based on the observation, the following oxidation mechanism is proposed. When NaCl crystals are adsorbed on Zry surface, the bonding between Zry and NaCl should delay the oxidation of the metal layer just beneath salt crystals. Compressive stress builds up in the oxide during oxidation, and the oxide near salt crystals relieves the compressive stress more easily, since metal or thinner oxide beneath the crystal easily deforms. As oxide thickens, relaxation of stress in oxide makes tension start to appear on the oxide surface, but it comes first on the sites around the salt crystals, where the compressive stress is already relieved. This non-uniform stress-relief mechanism can induce many cracks surrounding NaCl crystals. These cracks can supply open

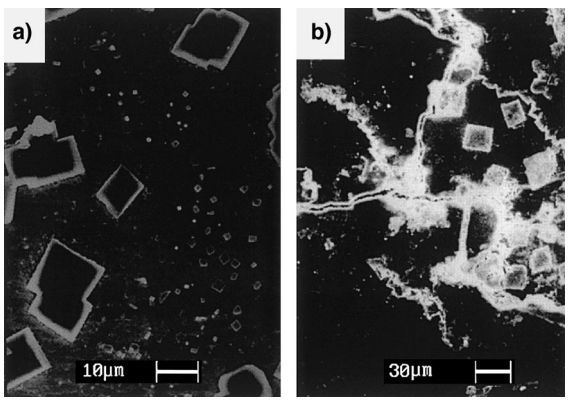

Fig. 12. (a) Zry surface after adsorption, (b) the surface after 36 h oxidation at 450°C in air.

paths to oxygen to inner oxide, and oxidation should be enhanced. The crack length is dependent on the size of NaCl crystals. Abnormally porous oxide regions are also observed at the region where tiny NaCl crystals were occupied. The parabolic rate law may come from crack-enhanced oxidation, i.e., the cracks formed near salt crystals expand their length and depth, resulting in enhancement of the oxidation. Cl ion in the oxide layer makes the oxide brittle, and helps cracking.

NaCl was also adsorbed on the post-transition oxide layer and tested. The results at 450°C are shown in Fig. 5. NaCl on the oxide layer still enhances oxidation. Fig. 13 shows the surface of specimens during the experiment. Several size salt crystals are observed on the surface initially (Fig. 13(a)). After 146 h oxidation at 450°C in air, salt crystals become smaller and seem to diffuse into oxide (Fig. 13(b)). Salt crystals disappear and look vague on the surface after 434 h oxidation (Fig. 13(c)). Kofstad suggests chlorine migrate through the scale as chlorine molecules or atoms, not in the form of chloride ions, due to the fact that there is considerably more chloride at the metal/scale interface than at the scale surface. After chlorine molecules are formed from NaCl, there leave Na_2O in dry air and NaOH in humid air [36]. We examined NaCl crystals at 450°C in air for weeks; but, any noticeable change in weight or shapes was not detected. Thermodynamic study indicates very low possibility of chloride vapor formation [28,29]. Hence, disappearance of NaCl crystals on the surface cannot be explained by evaporation only. The oxidation rate of the specimen was enhanced after the adsorption of NaCl on the oxide layer, which indicates NaCl (or Cl) certainly affects newly formed oxide. It is quite puzzling that ionic crystals (NaCl) move into another ionic solid (ZrO_2) with such a fast speed at 450°C, which is too low temperature to be explained in diffusion.

Cl is notorious for accelerating the oxidation of metals. Major role of Cl in enhancement of oxidation of Zry seems embrittlement of oxide. Embrittled oxide makes many cracks grow into the inner oxide, and may reach up to near the oxide–metal interface. There must be many microcracks that enhances oxidation and transport of NaCl (or Cl), based on the enhanced oxidation rate. Unusual diffusion like surface diffusion along the microcracks is suspected. However, the fast dissolution of NaCl into ZrO_2 is an open question, and needs more study.

Fluorides were also adsorbed on the oxide surface of Zry and reoxidized to see the effect of adsorbed dirt. NaF is the most powerful oxidation-enhancer among the adsorbates tested in the experiment. Fig. 14 shows the surface of the specimens. There appear many cracks (and even spalling) on the surface of NaF-adsorbed specimen oxidized up to 108 h (Fig. 14(a)). KF adsorbed specimen shows spalling at the oxide surface, but crack density seems lower than NaF-adsorbed one (Fig. 14(b)). Cl and F are known to make oxide very brittle. Assuming that only fluorine ion changes the oxide property, the dissolution rate of fluoride in oxide is the important factor controlling the oxidation rate of Zry. NaF seems to dissolve faster in oxide than KF does. LiF on the oxide surface barely dissolve into oxide. Most LiF on the surface stays after enough time of oxidation (Fig. 14(c)), and LiF does not affect the oxi-

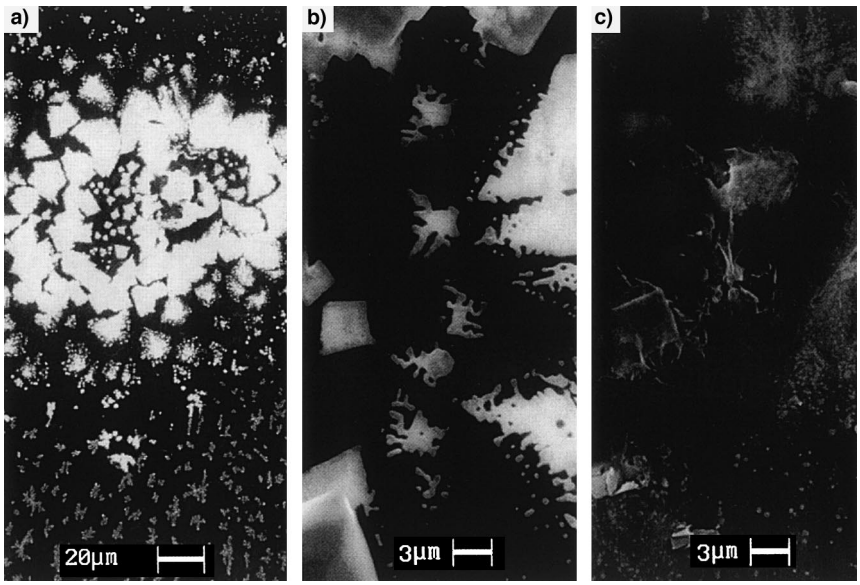

Fig. 13. Surface of NaCl adsorbed specimens. (a) after adsorption, (b) 146 h oxidation at 450°C, (c) 434 h oxidation at 450°C.

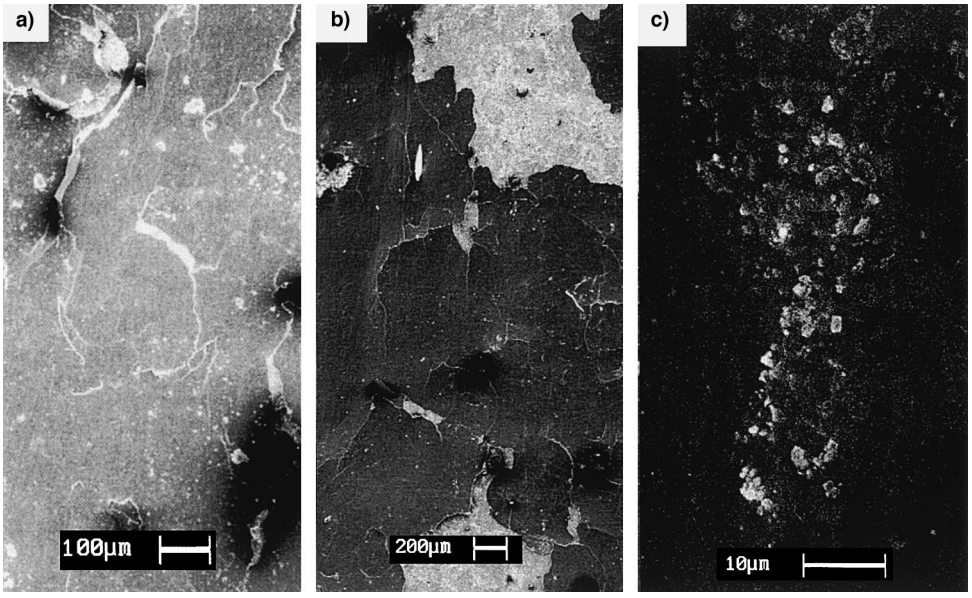

Fig. 14. Surface of fluoride adsorbed specimens. (a) NaF adsorbed, (b) KF adsorbed, (c) LiF adsorbed specimen.

dation of Zry. The origin of the difference in dissolution rates among these fluorides on the growing zirconia layer is also an interesting problem, and open to question.

5. Conclusion

To see the effects of adsorbates on Zry oxidation in the accident condition and in dry storage condition, commercially used Zircaloy-4 tube specimens with adsorbates on the surface were oxidized in dry atmosphere. The effects are quite diverse depending on the type of adsorbates, the atmosphere, and conditions. They are summarized in Table 4.

LiOH works as a mineralizer stabilizing monoclinic phases (enhancing allotropic transformation of tetragonal to monoclinic phase), and makes the finer oxides during the oxidation in air and in steam. At the low temperature, rapid transformation to monoclinic phases makes many fast diffusion paths to oxygen, like microcracks and micro open pores. In air oxidation, the portion of tetragonal oxides is quite high in the pre-transition oxide layer, so the local and non-uniform rapid-transformation makes damages in oxide layer resulting in enhancement of oxidation. In steam oxidation, H in steam is another mineralizer, so LiOH effect is not so effective as that in air oxidation. At the high temperature, tetragonal phases exist in oxide layer at least in the pre-transition stage. LiOH stabilizes monoclinic phases that have an order lower oxygen diffusion coefficient than tetragonal oxides. The early and fully developed monoclinic oxides slower the oxidation. H_3BO_3 retards the role of LiOH by making microcracks distributed just in between locally distributed LiOH region.

NaCl on pickled surface enhances oxidation by making cracks induced from non-uniform stress-relaxation in the oxide around NaCl crystals. Oxidation kinetics depends on the growth rate of crack. NaCl on post-transition oxide layer also enhances oxidation. NaCl on the surface dissolves fast into inner oxide. NaCl (or Cl) damages also newly born oxides, and micro-

Table 4
The summary of the experimental results performed in this study

Atmosphere	Adsorption surface or condition	Adsorbates	Effects on oxidation
Air	Pickled surface	LiOH, NaCl	Increase
	Post-transition oxide layer	NaCl, NaF, KF	Increase
		LiOH, LiF	No or Negligible
Steam	High temp.(>700°C)	LiOH	Slight Decrease
		LiOH-H_3BO_3	No or Negligible
	Low temp.(<500°C)	LiOH	Slight Decrease

cracks can reach up to metal–oxide interface resulting in enhancement of oxidation. The effects of fluorides are similar to NaCl, but the extent of enhancement is greater in the case of NaF and KF. NaF turned out to be most harmful adsorbate tested in the experiment, and KF follows after. LiF does not enhance the oxidation. F changes the oxide to be brittle. The dissolution of fluoride in oxide seems to decide the degree of oxidation enhancement. Fast dissolution of NaCl and fluorides in growing Zry oxide is open to question.

References

[1] A.B. Johnson, E.R. Gilbert, PNL-4835, 1983.
[2] B. Cox, Oxidation of Zirconium and Its Alloy, in: Advances in Corrosion Science and Technology, Plenum, New york, 1976.
[3] J.K. Dawson, G. Long, W.E. Seddonand, J.F. White, J. Nucl. Mater. 25 (1968) 179.
[4] R.A. Ploc, J. Nucl. Mater. 82 (1975) 316.
[5] F. Gazarolli, R. Manzel, S. Reshke, E. Tenckhoff, Review of Corrosion and Dimensional Behavior of Zircaloy under Water Reactor Conditions, ASTM STP 681, 91 (1979).
[6] F. Gazarolli, D. Jorde, R. Mansel, J.R. Politano, P.G. Smerd, Waterside Corrosion of Zircaloy-Clad Fuel Rods in a PWR Environment, ASTM STP 754, 430, (1982).
[7] F. Gazarolli, H. Seidel, R. Tricot, J.P. Gros, Oxide Growth Mechanism on Zirconium Alloys, ASTM STP 1132, 395, (1991).
[8] R.E. Pawel, J.V. Cathcart, J.J. Campbell, J. Electrochem. Soc. 126 (1979) 1105.
[9] V.F. Urbanic, T.R. Heidrick, J. Nucl. Mater. 75 (1978) 251.
[10] S. Leistikow, G. Schanz, Nucl. Eng. Design 103 (1987) 65.
[11] T. Furuta, S. Kawasaki, J. Nucl. Mater. 105 (1982) 119.
[12] J.T. Prater, E.L. Courtright, ASTM STP 939, 1987, p. 489.
[13] M. Suzuki, S. Kawasaki, J. Nucl. Mater. 140 (1986) 32.
[14] ASTM-G2-88, Standard Test Method for Corrosion Testing of Products of Zirconium, Hafnium and their Alloys in Water at 680F or in Steam at 750F, Annual Book of ASTM Standards, 1992.
[15] E. Hillner, J.N. Chirigos, The Effect of Lithium Hydroxide and Related Solutions on the Corrosion Rate of Zircaloy in 680F Water, WAPD-TM-307, 1962.
[16] N. Ramasubramanian, P.V. Balakrishnan, Aqueous Chemistry of Lithium Hydroxide and Boric Acid and Corrosion of Zircaloy-4 and Zr-2.5 Nb Alloys, ASTM STP 1245, 378, 1994.
[17] B. Cox, M. Ungurelu, Y.M. Wong, C. Wu, Mechanisms of LiOH Degradation and H_3Bo_3 Repair of ZrO_2 Films, ASTM STP 1295, 114 (1996).
[18] D. Pecheur, J. Godlewski, P. Billot, J. Thomazet, Microstructure of Oxide Films Formed during the Waterside Corrosion of the Zircaloy-4 Cladding in Lithiated Environment, ASTM STP 1295 94 (1996).
[19] Y. Kato, M. Asano, T. Harada, Y. Mizutani, J. Nucl. Mater. 203 (1993) 27.
[20] N. Ramasubramanian, N. Precoanin, V.C. Ling, Lithium Uptake and the Accelerated Corrosion of Zirconium Alloys, ASTM STP 1023, 187 (1989).
[21] F. Garzarolli, J. Pohlmeyer, S. Trap-Pretsching, H.G. Weidinger, Proceedings I.A.E.A. Technical Committee Meeting on Fundamental Aspects of Corrosion of Zirconium-Base Alloys in Water Reactor Environments, IWGFPT/34, ISSN, 1990, 1011–2766.
[22] C.H. Hsueh, A.G. Evans, J. Appl. Phys. 54 (1983) 6672.
[23] J. Stringer, Corros. Sci. 10 (1970) 513.
[24] D. Whitney, J. Am. Ceram. Soc. 45 (1962) 612.
[25] H. Anada, K. Takeda, Microstructure of Oxides on Zircaloy-4, 1.0 Nb Zricaloy-4, and Zircaloy-2 Formed in 10.3 Mpa Steam at 673 K, ASTM STP 1295, 35 (1996).
[26] B. Cox, J.P. Pemsler, J. Nucl. Mater. 28 (1968) 73.
[27] J. Godlewski, G.P. Gros, M. Lambertin, J.F. Wadier and H. Weidinger, Raman Spectroscopy Study of the Tetragonal-to-Monoclinc Transition in Zirconium Oxide Scales and Determination of Overall Oxygen Diffusion By Nuclear Macroanalysis of O^{18}, ASTM STP 1132, 416 (1991).
[28] W.R. Smith, R.W. Missen, Chemical Reaction Equilibirum Analysis, in: Theory and Algorithms, Wiley, New York, 1982, p. 278.
[29] I. Barin, Thermochemical Data of Pure Substances, VCH, 1989.
[30] K. Park, D.R. Olander, J. Electrochem. Soc. 138 (1991) 1154.
[31] R.E. Pawel, J. Electrochem. Soc. 126 (1979) 1111.
[32] T. Smith, J. Electrochem. Soc. 112 (1965) 560.
[33] P. Kofstad, High Temperature Corrosion, chap. 9, Elsevier, New York, 1988.
[34] J.B. Lightstone, J.P. Pemsler, Mater. Sci. Res. 4 (1969) 461.
[35] J.L. Hart, A.C.D. Chaklader, Mater. Res. Bull. 2 (1962) 521.
[36] P. Kofstad, High Temperature Corrosion, chap. 14, Elsevier, New York, 1988.